

EARLY COMMISSIONING OF THE LUMINOSITY DITHER SYSTEM FOR SUPERKEKB*

Y. Funakoshi[†], T. Kawamoto, M. Masuzawa, S. Nakamura, T. Oki, M. Tobiyaama, S. Uehara,
R. Ueki, KEK 305-0801 Tsukuba, Japan
A. S. Fisher, M. K. Sullivan, D. Brown, SLAC, 94025 Menlo Park, U.S.A.
U. Wienands, ANL 60439 Argonne, U.S.A.
P. Bambade, S. Di Carlo, D. Jehanno, C. Pang, LAL, 91898, Orsay, France
D. El Khechen, CERN, CH-1211, Geneva, Switzerland

Abstract

SuperKEKB is an electron-positron double ring collider at KEK which aims at a peak luminosity of $8 \times 10^{35} \text{cm}^{-2}\text{s}^{-1}$ by using what is known as the “nano-beam” scheme. A luminosity dither system is employed for collision orbit feedback in the horizontal plane. This paper reports a system layout of the dither system and algorithm tests during the SuperKEKB Phase 2 commissioning.

INTRODUCTION

The SuperKEKB collider [1] employs a luminosity dither system that was used at SLAC for PEP-II [2] [3] for maintaining the horizontal offset of the two beams at the IP and maximizing luminosity. For this purpose, a collision orbital feedback based on the beam-beam deflection was used in both vertical and horizontal planes at KEKB. With the “nano-beam” scheme, however, the horizontal beam-beam parameters are much smaller than those at KEKB, and detecting a horizontal orbit offset at IP using the beam-beam deflection is not effective at SuperKEKB. Therefore, a dithering method was introduced for SuperKEKB. A good collision condition is sought for by dithering the positron beam (LER, Low Energy Ring), and once a good collision condition is found, it is maintained by an active orbital feedback, which moves the electron beam (HER, High Energy Ring) relative to the LER by creating a local bump at the IP. The algorithm of the system is described elsewhere [4]. The dither system was tested with colliding beams in the SuperKEKB Phase 2 commissioning.

DITHERING SYSTEM

System Layout

The block diagram of the dither system is shown in Fig. 1. The system consists of fast luminosity monitors, a lock-in amplifier, coils for dithering, a programmable amplifier whose functions are gain and phase adjustments for each power supply, actuators (a bump system called “iBump system” which is also used for the fast vertical feedback), a controller for the iBump system, a dither control system (the actual feedback algorithm will be run in an IOC on a PLC) and power supplies of the dithering coils. Those devices are distributed

three different locations, *i.e.* a beam line in the SuperKEKB tunnel, Tsukuba B4 control room which is located near the beam line and Belle 2 Electronics Hut where the Belle 2 data acquisition electronics are assembled. PLC and the iBump system are connected through the EPICS control network and the whole dither system is control by the EPICS system. The system is also connected to the SuperKEKB center control room through the network and can be monitored and controlled therefrom.

Dither Coils

Eight sets of Helmholtz coils for the dithering system were designed and fabricated and their magnetic properties were measured at SLAC [5]. The coils were installed in the SuperKEKB tunnel in June 2015. Each set consists of a pair of coils to provide a horizontal kick and/or another pair of coils to provide vertical kick to the positron beam. The coils are designed to be mounted on the vacuum pipes directly. The coils are installed at 8 locations in the LER, 4 on the right side of the IP (ZD1RP, ZD2RP, ZD3RP and ZD4RP) and another 4 on the left side (ZD1LP, ZD2LP, ZD3LP and ZD4LP), as is shown in Fig. 2. Three types of coils are needed to be designed as the cross sections of the beam pipes vary by location. Two types (ZD1L/RP, ZD2L/RP) are symmetric in shape and have both horizontal and vertical coils while the third type (ZD3L/RP and ZD4L/RP) is asymmetric as this type is mounted on the vacuum pipe ante-chamber and have coils for the vertical kick. Field harmonics were evaluated by a rotating coil system, shown in Fig. 3. The required field uniformity of 0.1% is achieved over a range of ± 10 mm, even with the asymmetric type coil. The LER beam is kicked sinusoidally by the coils in the horizontal direction around the IP at a frequency of 79 Hz. The coils for vertical kick are prepared in order to correct the x-y coupling in the IP bump region.

Luminosity Monitor

Two types of fast luminosity monitors are used for studying dither. They both detect photons, re-coiled electrons, or positrons from radiative Bhabha scattering in the very forward (“zero degree”) direction. One monitoring system is called zero degree luminosity monitor (ZDLM) and is based on Cherenkov and scintillation counters [6]. The other system is developed by LAL, which uses diamond sensors and is called “LumiBelle2” [7]. Required accuracy of the

* Work supported by U.S.-Japan Science and Technology Cooperation Program in High Energy Physics.

[†] yoshihiro.funakoshi@kek.jp

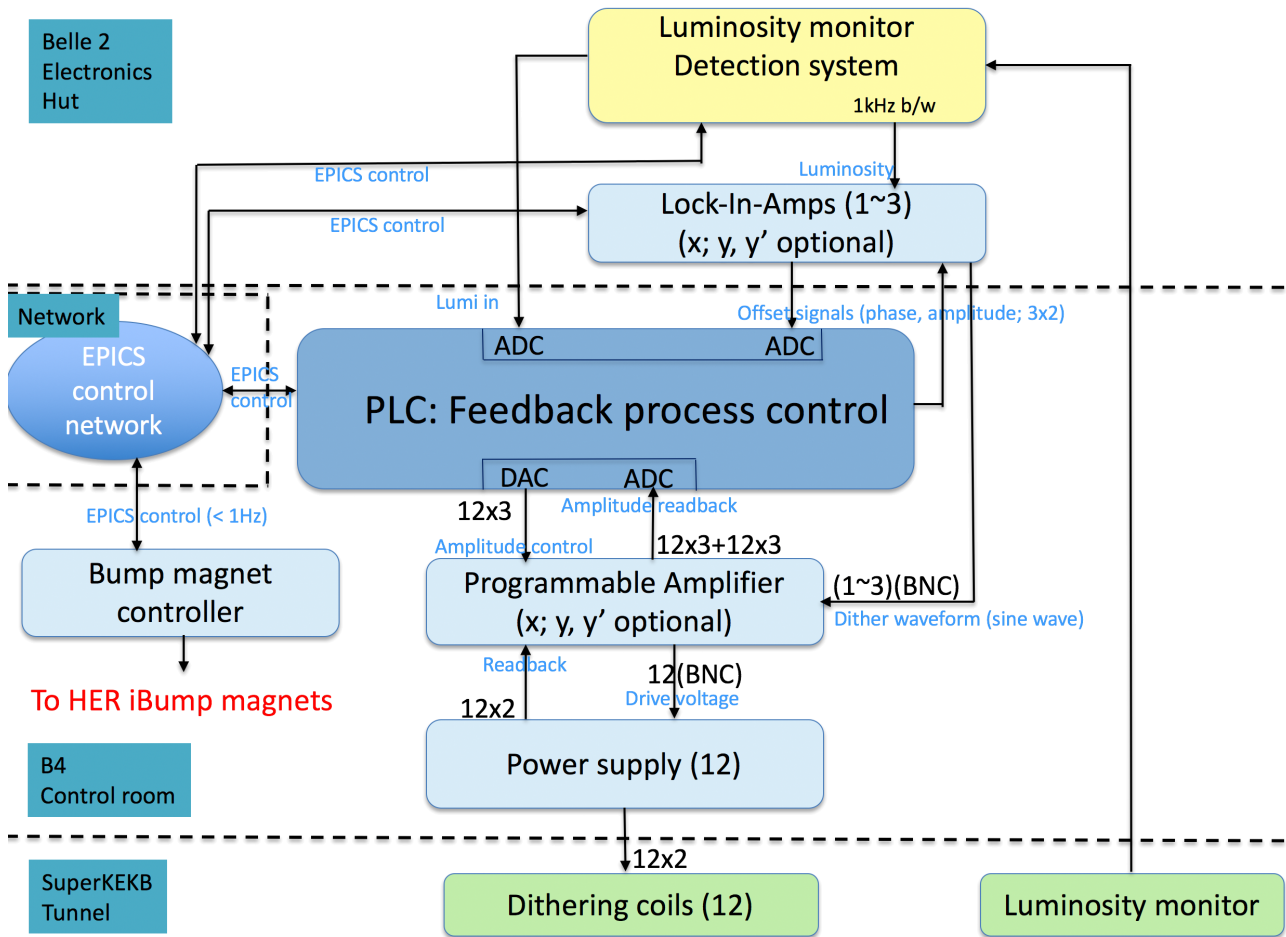


Figure 1: A block diagram of the dither feedback system.

luminosity monitor has been studied by a simulation and is 1% at 1 kHz. The short latency of 1 ms is required so that the monitor can detect a luminosity deviation at a high frequency.

Other Hardwares

A lock-in amplifier (AMETEK ADVANCED MEASUREMENT TECHNOLOGY model 7230) is used to generate a sine wave at a dither frequency. We chose 79 Hz as the dither frequency to avoid interference from the 50-Hz power line and injection frequencies of 1, 2, 5, 12.5, and 25 Hz. The sine wave is used as an input to the power supplies via a programmable amplifier. The luminosity signals are input to the lock-in amplifier, which mixes them with the reference dither signal and then low-pass filtering to provide an output voltage proportional to the dither frequency component of the luminosity together with a phase relation between the dither sine wave and the luminosity modulation signal. The dither feedback acts so that the output of the lock-in amplifier becomes minimum. The programmable amplifier was also designed and fabricated by SLAC [5]. The time delay was adjusted through the programmable amplifier by using the phase-shifter. The fudge factors of each

coil were obtained by analyzing the actual beam orbit. They were used to improve closure of the bump orbit during beam commissioning.

BEAM TEST AND COMMISSIONING

This section summarizes the results from the dithering study with colliding beams. The luminosity signals from ZDLM and LumiBelle2 were used as input to the lock-in amplifier.

Response of Lock-in Amplifier to Luminosity Modulation

We checked the response of the lock-in amplifier twice, *i.e.* on May 5th and July 14th. Figure 4 and 5 show results on May 5th. In the measurement the vertical beta function at the IP was 8mm for both rings and the luminosity was less than $10^{32} \text{cm}^{-2} \text{s}^{-1}$. The dither amplitude at the IP was $40 \mu\text{m}$. The output voltage from the lock-in amplifier (magnitude) and the phase are plotted as a function of the horizontal offset at the IP for ZDLM and LumiBelle2. The lock-in amplifier accepts two inputs; Input A for ZDLM and Input B for LumiBelle2 and the polarity of Input B is inverted in the lock-in amplifier. That is why the sign of the phases for the

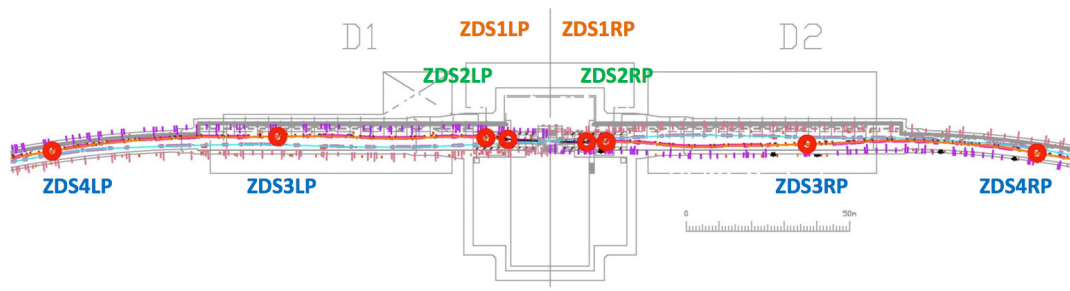


Figure 2: Locations of the dithering coils. Three different types of coils are indicated by three different colors.



Figure 3: Ante-chamber type dithering coil is being measured by a rotating system.

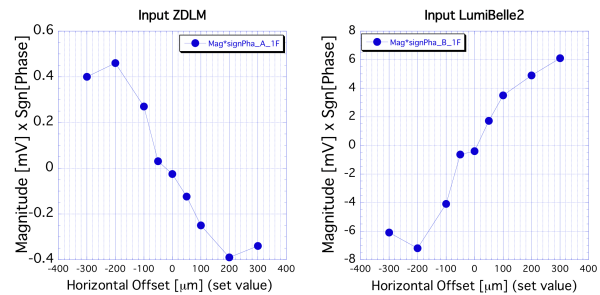


Figure 5: Magnitude times Sgn[phase] is plotted against the horizontal offset at IP for ZDLM (left) and LumiBelle2 (right). The same data as Fig. 4 are used.

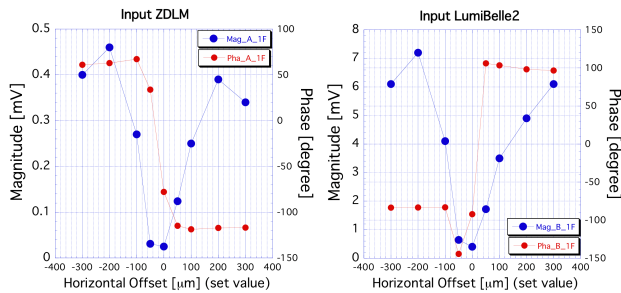


Figure 4: Magnitude (blue) and phase (red) from Lock-in Amp are plotted against the horizontal offset at IP for ZDLM (left) and LumiBelle2 (right).

two inputs is opposite in Fig. 4. The horizontal offset at the IP was created by making horizontal bump orbits at the IP in HER. In this measurement, the dependence of the luminosity on the horizontal offset was not clear in the scan range in the figures, since the IP vertical beta function was not so small and the luminosity was not very high. Nevertheless, the phase jump at around the zero offset was clearly seen in the scan. This shows superiority of this dither method using the lock-in amplifier. In Fig. 5, the product of the magnitude and the sign of the phase using the same data as in Fig. 4 is plotted as a function of the horizontal offset at IP. In the luminosity feedback routine, the quantity shown in Fig. 5 is used as an input value. The feedback acts so as to find the zero cross point of the input and keep it by using the PI algorithm.

The second measurement was done on July 14th. In the measurement the vertical beta function at the IP was 3mm for both rings and the luminosity was around $10^{33} \text{cm}^{-2} \text{s}^{-1}$. The dither amplitude at the IP was $20 \mu\text{m}$. Four data sets

were taken using LumiBelle2 and ZDLM alternatively as input to the lock-in amplifier, with varying HER horizontal orbit bump height at the IP, as was done on May 5th. Table 1 summarizes the procedure of the scans. The output voltage (magnitude) from the lock-in amplifier is plotted as a function of the horizontal beam position at QC1LE in Fig. 6 for scans 3 and 4, where the ZDLM signal was used as input to the lock-in amplifier. Here, QC1LE is a final focus quadrupole magnet for the electron ring on the left side of the IP and the beam position is measured value at the BPM attached on the IP side of the magnet. The output voltage becomes zero and the phase jump takes place at $x = -0.95 \text{ mm}$ in both scans, which are consistent with the position of the luminosity peak as is shown below. The plots of the magnitude and the phase for scans 1 and 2 are shown in Fig. 7, where LumiBelle2 was used as input to the lock-in amplifier. When the magnitude is zero, or close to zero, phase jump occurs. However, the beam position is not at $x = -0.95 \text{ mm}$ but at $x = -1.05 \text{ mm}$. This does not match the beam position where luminosity peaks as is shown below. The magnitude curve is not symmetric with respect to its minimum either, which is not the case with scans 3 and 4. The cause of this mismatch and asymmetric behavior will be investigated during Phase 3 that is scheduled to start in the spring of 2019. Also in this measurement on July 14th, two inputs of the lock-in amplifier are used for ZDLM and LumiBelle2. However, the sign of the phase for the two inputs is same as seen in Figs. 6 and 7, since we set phase offsets properly.

Content from this work may be used under the terms of the CC BY 3.0 licence (© 2018). Any distribution of this work must maintain attribution to the author(s), title of the work, publisher, and DOI.

Table 1: Summary of Horizontal Scan (July 14th)

| | Input to lock-in amplifier | Scan range (μm) |
|-------|----------------------------|------------------------------|
| Scan1 | LumiBelle2 | -250 \rightarrow +250 |
| Scan2 | LumiBelle2 | +250 \rightarrow -250 |
| Scan3 | ZDLM | -150 \rightarrow +150 |
| Scan4 | ZDLM | +150 \rightarrow -150 |

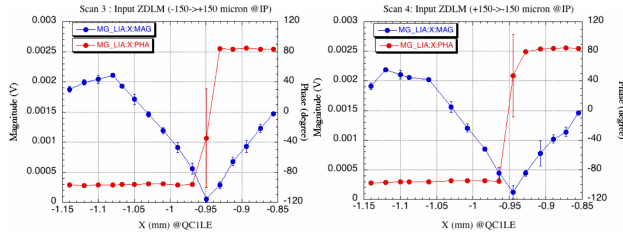


Figure 6: Magnitude (blue) and phase (red) are plotted against the HER beam position x for scans 3 (left) and 4 (right).

Luminosity Response

Figure 8 shows the luminosity response when the bump height at the IP was changed during scan 3, as an example. The luminosity is normalized to its peak for each luminosity monitor. The normalized luminosity is fitted by the following Gaussian functions:

$$L_0 = m_1 + \exp\left(-\frac{(x - m_2)^2}{2m_3^2}\right) \quad (1)$$

where x is the beam position monitored by the beam position monitor (BPM) at QC1LE. The fitted parameters m_2 and m_3 represent the HER beam position where the luminosity peaks and exhibits standard deviation, respectively. Table 2 summarizes the fitted parameters. Luminosity peaks when the HER beam position measured at QC1LE is -0.95 mm for all scans, indicating that the effects of the bump magnet hysteresis and drift of the beam orbits are negligible.

In the Eq. (1), the parameter m_3 corresponds to Σ_x^* for the usual collision scheme. In the "nano-beam scheme", however, we have to use an effective horizontal beam size σ_x^{*eff} instead of the actual horizontal beam size σ_x^* in the

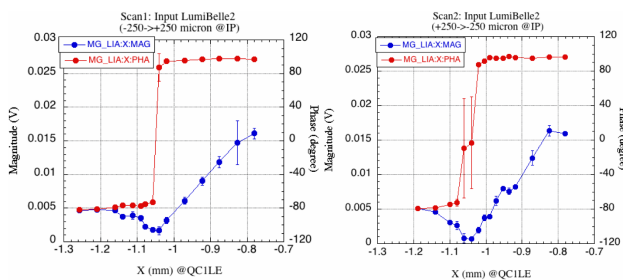


Figure 7: Magnitude (blue) and the phase (red) are plotted against the HER beam position x for scans 1 (left) and 2 (right).

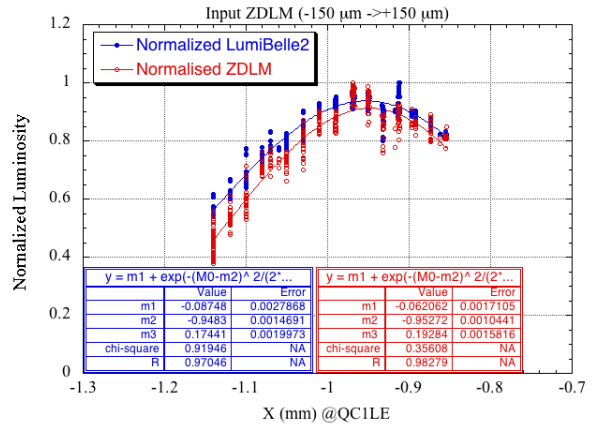


Figure 8: Luminosity is plotted against the beam position measured at the QC1LE BPM during scan 3.

Table 2: Summary of Gaussian-fitted parameters

| Detector | LumiBelle2 | | ZDLM | |
|----------|------------|------------|------------|------------|
| | m_2 (mm) | m_3 (mm) | m_2 (mm) | m_3 (mm) |
| Scan 1 | -0.94 | 0.27 | -0.95 | 0.24 |
| Scan 2 | -0.94 | 0.21 | -0.95 | 0.18 |
| Scan 3 | -0.95 | 0.17 | -0.95 | 0.19 |
| Scan 4 | -0.94 | 0.20 | -0.95 | 0.18 |

calculation of the luminosity or the beam-beam parameters. The effective horizontal beam size is denoted as follows:

$$\sigma_x^{*eff} = \sigma_z \sin \phi_c \quad (2)$$

where ϕ_c and σ_z are the half crossing angle at the IP (41.5 mrad at SuperKEKB) and the bunch length, respectively. The bunch length was measured to be 5.5 mm for both LER and HER when the bunch current is 0.3 mA [8]. Using 41.5 mrad for ϕ_c and 5.5 mm for σ_z , we obtain ~ 0.23 mm for σ_x^{*eff} and Σ_x^{*eff} is calculated as ~ 0.33 mm. This is $\sim 60\%$ larger than m_3 in Table 2. Luminosity degraded more than expected with a horizontal offset. This can be explained by considering the hourglass effect. When there is a crossing angle at the IP as is in SuperKEKB, a horizontal offset shift introduces a collision point shift in the beam direction, as is indicated in the left side drawing in Fig. 9. The vertical beta-function (β_y) is plotted on the right side. A 100 μm horizontal offset makes β_y larger, which degrades luminosity by approximately 7.2% with β_y^* of 3 mm. If a horizontal offset causes beam blow-up at the IP, an additional degradation in luminosity may take place.

Dither Feedback

A feedback algorithm using the PI control was first tested in May 10th. The magnitude from the lock-in amplifier and the bump height at the IP are plotted in Fig. 10. In this test, we used LumiBelle2 for the input to the lock-in amplifier. The feedback algorithm loop runs in the operation computer system connected through the network in this Phase 2 test.

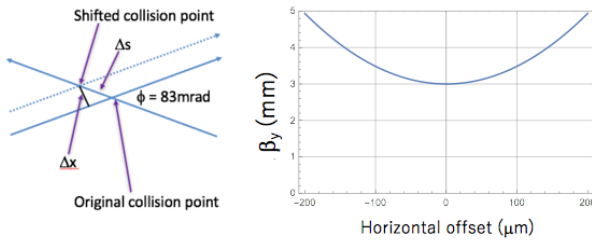


Figure 9: Hourglass effect when there is a horizontal offset at the IP.

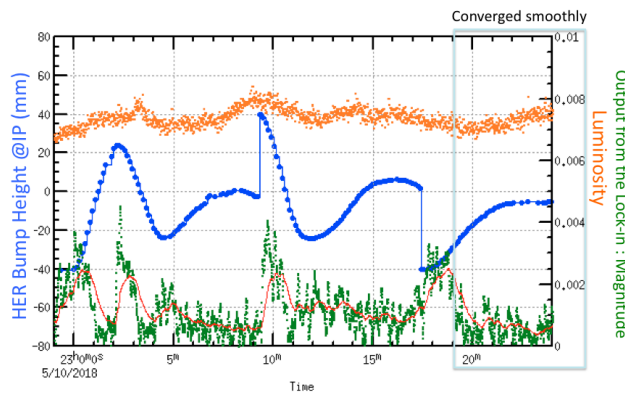


Figure 10: Magnitude (green) and bump height at the IP (blue) are plotted with luminosity (orange) during the dither feedback test.

The feedback cycle was ~ 8 s, which was mainly determined by a data accumulation time in the lock-in amplifier. In the test, the luminosity was around $1 \times 10^{32} \text{cm}^{-2} \text{s}^{-1}$ and we needed a relative long accumulation time for the lock-in amplifier. It determines a proper size and direction of the offset at the IP in the HER. These parameters are then sent to the iBump control system via EPICS to create a bump in the HER. The feedback loop set a bump in the correct direction and made the output from the lock-in amplifier smaller, though there were a couple of overshoots initially. After finding a good feedback parameter set, the feedback converged smoothly to an optimum value without any overshoot and the magnitude was brought to close to zero. The luminosity response was not clear this time, as β_y^* was relatively large (8 mm). The luminosity was not very sensitive to the horizontal beam offset in this test.

SUMMARY AND FUTURE PROSPECTS

The dither feedback system finds the optimum horizontal offset between the LER and HER to maximize luminosity by determining the minimum magnitude of the output of the lock-in amplifier. In the test on July 14th, the optimum horizontal offset was found successfully when ZDLM was used as input to the lock-in amplifier. There was a shift of approximately $100 \mu\text{m}$ between the luminosity maximum offset and the magnitude minimum offset when LumiBelle2 was used as input. This will be investigated during the Phase 3 run first. The test of the dither feedback using LumiBelle2 as input on May 10th was successful. The dependence of luminosity on the horizontal offset agrees with the prediction estimated from the crossing angle, bunch length, horizontal beam size at the IP, and hourglass effect. In the beam operation in Phase 2, the dither feedback was not needed, since the dependence of the luminosity on the horizontal offset was weak. In Phase 3, however, the dither feedback would become indispensable with smaller values of β_y^* .

REFERENCES

- [1] T. Abe *et al.*, "SuperKEKB design report", in preparation, to be published in KEK Report.
- [2] S. Gierman *et al.*, "New fast dither system for PEP-II", in *Proc. EPAC'06*, Edinburgh, GB, June 2006, pp. 652-654.
- [3] A.S. Fisher *et al.*, "Commissioning the fast luminosity dither for PEP-II", in *Proc. PAC'07*, Albuquerque, NM, USA, June 2007, pp. 4165-4167.
- [4] M. Masuzawa *et al.*, "Early Commissioning of the luminosity dither system for SuperKEKB", in *Proc. IBIC'18*, Shanghai, China.
- [5] U. Wienands *et al.*, "Dither coils for the SuperKEKB fast collision feedback system", in *Proc. IPAC'15*, Richmond, USA, May 2015, pp. 3500-3502.
- [6] T. Hirai, S. Uehara and Y. Watanabe, "Real-time luminosity monitor for B-factory experiment", *Nuclear Instruments and Methods in Physics Research*, Section A, pp. 670-676, 11 Feb., 2001.
- [7] S. Di Carlo *et al.*, "Early Phase 2 Results of LumiBelle2 for the SuperKEKB Electron Ring", in *Proc. IPAC'18*, Vancouver, Canada, April-May 2018, pp. 2934-2935.
- [8] H. Ikeda, private communications.

Content from this work may be used under the terms of the CC BY 3.0 licence (© 2018). Any distribution of this work must maintain attribution to the author(s), title of the work, publisher, and DOI.